Hydrol. Earth Syst. Sci. Discuss., 7, 8809–8835, 2010
www.hydrol-earth-syst-sci-discuss.net/7/8809/2010/
doi:10.5194/hessd-7-8809-2010

Hydrology and Earth System Sciences Discussions

Hydrological real-time modeling using remote sensing data

P. Meier, A. Frömelt, and W. Kinzelbach

ETH Zürich, Institute of Environmental Engineering (IfU), Wolfgang-Pauli Strasse 15, 8093 Zürich

Received: 28 October 2010 – Accepted: 2 November 2010 – Published: 10 November 2010

Correspondence to: P. Meier (meier@ifu.baug.ethz.ch)

Published by Copernicus Publications on behalf of the European Geosciences Union.

Abstract

Reliable real-time forecasts of the discharge can provide valuable information for the management of a river basin system. Sequential data assimilation using the Ensemble Kalman Filter provides a both efficient and robust tool for a real-time modeling framework. One key parameter in a hydrological system is the soil moisture which recently can be characterized by satellite based measurements. A forecasting framework for the prediction of discharges is developed and applied to three different sub-basins of the Zambezi River Basin. The model is solely based on remote sensing data providing soil moisture and rainfall estimates. The soil moisture product used is based on the back-scattering intensity of a radar signal measured by the radar scatterometer on board the ERS satellite. These soil moisture data correlate well with the measured discharge of the corresponding watershed if the data are shifted by a time lag which is dependent on the size and the dominant runoff process in the catchment. This time lag is the basis for the applicability of the soil moisture data for hydrological forecasts. The conceptual model developed is based on two storage compartments. The processes modeled include evaporation losses, infiltration and percolation. The application of this model in a real-time modeling framework yields good results in watersheds where the soil storage is an important factor. For the largest watershed a forecast over almost six weeks can be provided. However, the quality of the forecast increases significantly with decreasing prediction time. In watersheds with little soil storage and a quick response to rainfall events the performance is relatively poor.

1 Introduction

In hydrological forecasting, fully distributed, physically based models provide the ability to account both for the heterogeneity of a watershed and physical changes of the system (e.g. induced by the construction of irrigation schemes or land use change). On the other hand simple conceptual models can provide a satisfactory performance for

HESSD

7, 8809–8835, 2010

short term forecasts. Especially in regions with limited facilities for the measurement of relevant hydrological data this can be an advantage.

Kitanidis and Bras (1980a) stated that the effective water management in a river basin system needs a reliable real-time forecast. This involves a continuous correction of the forecasts based on the prediction errors of earlier forecasts. The application of a model is accompanied by several sources of errors, such as model, input and parameter uncertainty. This leads to a deficient knowledge of the system states. Hence it is appropriate to use observed system outputs to update the states of the system (Kitanidis and Bras, 1980a,b).

This so called data assimilation problem can be solved in different ways. In real-time applications a new assimilation problem is formulated at every time step. To solve this problem efficiently sequential assimilation techniques are considered superior (McLaughlin, 2002). Sequential assimilation algorithms, also known as filtering algorithms, are divided into two steps: first a propagation step, where the system states are propagated through time using a model and forcing data; second an update step, where the modeled states of the system are updated based on the difference between the modeled quantity and its real-world observation. To solve nonlinear filtering problems the Ensemble Kalman Filter (EnKF) has proven to be both efficient and robust (Evensen, 1994). EnKF has, other than standard batch calibration, the advantage of being able to incorporate a wide range of uncertainties. The uncertainties of forcing data, model parameters and modeled observations are considered separately but can be incorporated in the same mathematical scheme (Thiemann et al., 2001).

As soil moisture is a key parameter in land surface hydrology, the availability of area representative measurements offers a unique opportunity to improve hydrological modeling. The first global dataset on soil moisture has been presented by Wagner et al. (1999a). It was shown that runoff predictions were greatly enhanced when measured soil moisture both from ground measurements and from remote sensing were incorporated (Aubert et al., 2003; Crow and Ryu, 2009).

HESSD
7, 8809–8835, 2010

The assimilation of remotely sensed soil moisture data becomes more and more feasible. Several satellite missions have been launched or will be launched in the near future equipped with instruments to retrieve soil moisture using radar. These missions include the MetOp Advanced Scatterometer (ASCAT), the Soil Moisture and Ocean Salinity Mission (SMOS) and NASA's Soil Moisture Active-Passive instrument (SMAP) (Kerr et al., 2001; Naeimi et al., 2009; Piles et al., 2009).

This study presents a prediction framework for river discharge based solely on remotely sensed data of soil moisture and rainfall, a simple conceptual model and data assimilation techniques. The availability of the input data in real-time allows the model to be operated in real-time, providing a prediction for discharge each time new input data are retrieved. When observation data are available the model state is updated using sequential data assimilation techniques (EnKF). The update step allows the model to be relatively simple.

This modeling approach is evaluated in three different sub-basins within the Zambezi River basin (Fig. 1). The three watersheds are the Upper Zambezi upstream of the gauging station Senanga with an area of 281 000 km^2, the Kafue River where the discharge is measured at the Kafue Hook Bridge with an area of 95 300 km^2 and the Luangwa River which is gauged a few kilometers upstream of the confluence with the Zambezi River (142 070 km^2). These watersheds cover together more than one third of the whole Zambezi watershed and contribute more than one half of the total runoff at the mouth of the Zambezi, where the Upper Zambezi catchment contributes the largest amount (850 $m^3 s^{-1}$ mean annual discharge), the Kafue River discharges 300 $m^3 s^{-1}$ and the Luangwa River 700 $m^3 s^{-1}$.

The whole Zambezi River basin lies in the semi-arid zone of southern Africa. Rainfall is strongly seasonal and occurs almost exclusively between October and March. The total amount of rainfall is on average around 1000 $mm\,yr^{-1}$, the potential evapotranspiration around 2000 $mm\,yr^{-1}$.

The water resources in the Zambezi river basin are more and more developed. Feasibility studies for several new hydro-power plants are carried out and new irrigation schemes are developed all over the river basin. While the pressure on the resources is growing, short term forecasts of the discharge can help optimizing the operation of smaller reservoirs and water abstraction schemes for irrigation without neglecting the river dependent ecosystems as a third water user.

2 Soil moisture

The vadose zone is one of the most important components of the global water cycle. Through the coupling of water and energy fluxes soil moisture determines the local and global climate. However, the variability of soil moisture is very high in both space and time. Traditional measurement methods, such as TDR, are reasonably accurate but they provide information on a very local scale. Monitoring large areas is nearly infeasible. The typical correlation length for such measurements lies between a few tens of meters and a few hundred meters (Western et al., 2004). On larger scales the temporal variation seems to be very stable since it is mainly influenced by climatic conditions (Brocca et al., 2010). Therefore remotely sensed soil moisture data provides a valuable dataset for hydrological monitoring on a larger scale.

There is a wide variety of techniques measuring the soil water content through remote sensing. However, the data can only be retrieved by indirect measurements. Both active and passive methods rely on the measurement of radiation intensities in a certain range of wavelengths. For passive systems operating in the thermal infrared band the measurement target is the soil surface temperature (Verstraeten et al., 2006). The radiation intensity measured by systems operating in the microwave band is controlled by the dielectric constant of the top soil layer. Especially soil moisture products based on radar satellite imagery provide an attractive source for data since the influence of cloud cover and changing atmospheric conditions is minimal. Although they are governed by the same physical principles, generally three types of microwave techniques are distinguished: Passive radiometry and the two active methods using synthetic aperture radar (SAR) and radar scatterometer (Wagner et al., 2007). SAR

HESSD
7, 8809–8835, 2010

systems, providing data with a high spatial resolution, show a good performance over bare soils. Despite the significantly lower resolution, the multiple antenna configuration of scatterometers can facilitate the data processing to reduce the influence of vegetation on the signal (Baghdadi et al., 2008).

Recent studies have shown the usefulness of radar scatterometer derived soil moisture data for hydrological applications. Even with the generally coarse resolution these data can be applied successfully for hydrological modeling since small scale spatial variability of the soil water content is averaged within the scatterometer footprint (Ceballos et al., 2005; Scipal et al., 2005).

In this study the dataset of soil moisture derived from the radar scatterometer on board the two ERS satellites is used (Wagner et al., 1999b). The ERS radar scatterometers are operating in the C-band at a frequency of 5.3 GHz using three sideways-looking antennas arranged at an angle of 45 degrees.

The measured back-scattering intensity is dependent on different properties of the surface, mostly on the surface roughness, the vegetation and the soil moisture. Generally wet soil results in higher back-scattering intensity than a dry soil. Since the arrangement of the antennas allows to rule out the effects of vegetation and the surface roughness can be considered to be constant over time, the dry and the wet state of each pixel can be determined using a change detection algorithm (Wagner et al., 1999a).

Since the electromagnetic waves in the bandwidth only penetrate the top few centimeters of the soil, the soil column water content for large depths has to be estimated. Wagner et al. (1999b) proposed a method to calculate a so called Soil Water Index (SWI) based on a simple two-layer moisture balance model. It computes a weighted average of the past measurements using an exponential filter of the form $\exp(\frac{-t}{T})$ and is therefore acting as a low-pass filter. The time after which the weight for a single measurement has declined by one half is globally set to 14 days. The dataset used in this study provides SWI data at a 10-daily time step. Scipal et al. (2005) concluded that even this low resolution soil moisture data can be applied in hydrological modeling.

HESSD
7, 8809–8835, 2010

The scatterometer based surface soil moisture data are strongly correlated to the occurrence of rainfall events but less correlated to the magnitude of these rainfall events (Fig. 2). In all three catchments the probability for a rainfall event to have taken place grows for higher soil moisture, whereas the amount of rainfall is mainly correlated to soil moisture when the soil has not yet reached a certain degree of saturation (around values of 0.8).

A similar effect can be observed if the correlation between the Basin Water Index (BWI) and the measured discharge is analyzed (Fig. 3). The BWI is calculated by averaging the SWI over the whole river basin (Scipal et al., 2005). The variation of the discharge is relatively small for low soil moisture values. If the values exceed 0.5 to 0.6 the variation suddenly increases. This indicates that the discharge is to some extent decoupled from the soil moisture as the soil approaches complete saturation. This decoupling is mainly caused by rainfall. Therefore modeling efforts which include rainfall data seem to be more realistic.

The analysis of the correlation also shows that to obtain the best correlation the discharge has to be shifted by very different time lags. Not surprisingly the largest watershed shows a long time lag of two months, whereas for the second largest watershed (Luangwa River) the time lag has to be set to zero to obtain an optimal fit. The optimal time lag for the Kafue River up to Kafue Hook Bridge is one month. These differences can be explained by the geological and geomorphological settings of the watersheds. The Luangwa River flows through the Luangwa Rift Valley which is an extension of the East African rift valley. The tributaries of the Luangwa drain the steep escarpment of the rift and therefore have a very short response time to rainfall. In addition to the more gentle slope of the drainage area, the two other watersheds feature at least one large wetland each which retards the flow of the water. The soil moisture product used is not very sensitive to the presence of wetlands. They therefore cause an additional retardation of the discharge which is mainly formed outside the wetlands.

HESSD
7, 8809–8835, 2010

A long time lag entails a long potential forecast period. Therefore a real-time model based on soil moisture data and rainfall is more powerful in terms of the forecast period in large watersheds.

3 Methodology

3.1 Data

Besides the soil moisture data which are described in the previous section, rainfall data are used as forcing data and measured discharge is applied for updating the model.

The rainfall dataset is provided by the Famine Early Warning Systems Network (FEWS NET) and can be downloaded free of charge from the internet. The data are available at a 10 days interval starting from July 1995. FEWS NET rainfall data incorporate various satellite based rainfall estimates and data measured at gauging stations (Herman et al., 1997). Since the soil moisture data used are available only up to January 2002 the period where soil moisture data and rainfall data overlap is only little more than six years.

Daily discharge data are available at the outlets of the three sub-basins. For the Kafue and the Luangwa sub-basin the data available cover the whole period where rainfall and soil moisture data are available simultaneously. The discharge of the Upper Zambezi sub-basin is measured from October 1996 only.

3.2 Soil moisture – runoff model

To model the discharge at the outlet of a basin a simple conceptual model was developed. The model consists of two compartments: a surface water storage and a subsurface water storage (Fig. 4). All input data of the model, the soil moisture and the rainfall, are averaged over the whole river basin. Hence, the spatial variability is not considered. The basin-averaged soil moisture is equivalent to the Basin Water Index

HESSD
7, 8809–8835, 2010

(BWI) introduced by Scipal et al. (2005). The model is based on the following balance equations:

$$I_{GW} = k_1 AR(t)(1 - \mathrm{BWI}(t)) \tag{1}$$

$$\frac{\Delta S_S(t)}{\Delta t} = k_1 AR(t) - I_{GW} - k_2 S_S(t-1) \tag{2}$$

$$\frac{\Delta S_{GW}(t)}{\Delta t} = \max(I_{GW} + k_3(\mathrm{BWI}(t) - \mathrm{BWI}(t-1))\ ;\ 0) - k_4 S_{GW}(t-1) \tag{3}$$

where S_S and S_{GW} are the surface storage volume and the subsurface storage volume, respectively, I_{GW} is the direct infiltration of rainfall to the subsurface storage, R is the average rainfall in the river basin, A is the total area of the watershed and k_i are the model parameters.

The storage compartments are considered to be single linear storages. Depending on the value of the BWI, a part of the rainfall is routed to the surface water storage whereas the remaining water volume is routed to the subsurface storage. If BWI is 0 all water is routed to the subsurface, if BWI is 1 all water is routed to the surface storage. The storage change in the subsurface is modeled through the measured change in soil moisture (BWI(t)–BWI($t-1$)). The sum of the rainfall routed to the subsurface and the measured change in soil moisture represent the recharge to the subsurface compartment which is not allowed to be negative in this model. For the surface runoff (Q_S) and the subsurface runoff (Q_{GW}) two different time lags $\Delta\tau_S$ and $\Delta\tau_{GW}$ are applied to calculate the total discharge according to Eq. (4).

$$Q(t) = Q_S(t - \Delta\tau_S) + Q_{GW}(t - \Delta\tau_{GW}) \tag{4}$$

with

$$Q_S(t) = k_2 S_S(t-1) \quad \text{and} \quad Q_{GW}(t) = k_4 S_{GW}(t-1).$$

HESSD
7, 8809–8835, 2010

A physical interpretation of the parameters assigns the parameter k_1 to the losses (through evaporation) of rainfall before it enters a storage. The parameter k_3 relates the BWI to the total volume of water stored in the subsurface zone. The two parameters k_2 and k_4 are the rates at which the linear storage compartments are depleted. These model parameters are calibrated by running the model in deterministic mode using the Levenberg-Marquardt algorithm (Marquardt, 1963).

The time lags ($\Delta\tau_S$ and $\Delta\tau_{GW}$) are mostly dependent on the size of the watershed. In this model the time lags are considered to be an integral multiple of the length of a single time step ($\Delta\tau = n\Delta t,\ n = 1,2,3,\ldots$). Due to the discrete nature of the time lag, the parameter identification is done in two steps. For different pairs of $\Delta\tau_S$ and $\Delta\tau_{GW}$ the model parameters k_i are calibrated. The set of time lags with the minimal root mean square error (RMSE) between the observed and the computed flow together with the corresponding k_i are then chosen as optimal parameter set. Since the input data used are available every ten days the time step Δt of the model was set to ten days.

For comparison the regression model developed by Scipal et al. (2005) was used. This model uses a logarithmic regression between soil moisture and discharge Eq. (5). It uses three parameters representing a baseflow (Q_0), a hydrometric scaling factor χ_Q and a time lag $\Delta\tau$.

$$Q(t) = Q_0 + \chi_Q \ln\left(\frac{\mathrm{BWI}_{\max}}{\mathrm{BWI}_{\max} - \mathrm{BWI}(t-\Delta\tau)}\right) \qquad (5)$$

To assess the overall quality of the model presented in this article it is run in deterministic mode, without the data assimilation step. The simulated discharges are compared to the measured ones by calculating the root mean squared error (RMSE) and the Nash-Sutcliffe efficiency (Nash and Sutcliffe, 1970). Furthermore, they are compared to the discharges simulated with the reference model Eq. (5).

HESSD
7, 8809–8835, 2010

3.3 Real-time modeling

Ensemble Kalman Filtering updates the state variables of a model by correcting them using the difference between the measured observation and its predicted value. The state variables which are updated are the two storage volumes S_S and S_{GW}. As observation data the measured discharge is used.

Observed discharge data are available on a daily basis. Since the temporal resolution of the model is 10 days, data assimilation is carried out in every time step.

For the real-time modeling framework an ensemble of randomly perturbed input and observation data are generated. The rainfall data ensemble is generated using the gamma distribution. The gamma distribution only needs two parameters ($\Gamma(k,\theta)$). The expected value of a gamma distributed random variable X is defined as $E(X) = k\theta$ and the standard deviation as $\sigma_X = \sqrt{k}\theta$. The standard deviation is set to a fixed value ($\sigma_R = 50$ mm) which reflects the uncertainty of the rainfall data product (Herman et al., 1997). Using the measured rainfall amount as expected value of the perturbed rainfall for each time step, the two parameters k and θ can be calculated. Based on these parameters the rainfall ensemble $\tilde{\boldsymbol{R}}_t$ at time t is generated according to Eq. (6).

$$\tilde{\boldsymbol{R}}_t = \begin{pmatrix} \tilde{R}_t^1 \\ \vdots \\ \tilde{R}_t^i \end{pmatrix}, \quad \text{with} \quad \tilde{R}_t^i \sim \Gamma(k,\theta) = \Gamma\left(\frac{R_t^2}{\sigma_R^2}; \frac{\sigma_R^2}{R_t}\right), \tag{6}$$

where R_t is the measured rainfall at time t.

For the uncertainty of the BWI the standard deviation is set to 0.025 according to the standard error found by Ceballos et al. (2005). For the observed discharge data the variance of the added noise is proportional to their magnitude with a standard deviation of 0.05 times the measured value, as the absolute measurement error of discharge measurements is generally considered to be dependent on the discharge itself. Both, the BWI and the discharge perturbations are considered to follow a Gaussian distribution.

HESSD
7, 8809–8835, 2010

To assess the possible accuracy of the forecast, the model is run off-line in adaptive mode for the historic time series from the years 1995 to 2002.

4 Results and discussion

The parameters for the developed model are calibrated for all three watersheds. To analyze the performance of the model it was assessed both in a deterministic modeling mode and in the real-time (but off-line) modeling mode.

The model parameters obtained by calibration in the deterministic mode are shown in Table 1. For the time lags one can see a similar dependency on the size and geomorphology of the different watersheds as it was already observed for the correlation analysis (Fig. 3). The Upper Zambezi catchment has by far the longest response time whereas the Luangwa river basin shows a relatively quick response.

The only model parameter that shows a distinct dependency on the area of a watershed is the parameter that correlates the BWI to the total volume of water stored inside the subsurface storage, k_3. One can assume that the wetlands present in the Upper Zambezi and the Kafue watersheds have a huge impact on the water storage capacity.

Parameter k_1 which mainly reflects the water losses through evapotranspiration not only depends on the soil properties of the watershed but also on the average retention time in the catchment. The longer water is stored in a watershed the more evapotranspiration can be expected. The Upper Zambezi basin shows indeed the lowest value for k_1. The Kafue River basin shows a very similar value of k_1 which leads to the conclusion that the soil properties in the two basins are similar and that the influence of the size of a watershed on the parameter is marginal. While the area of the Luangwa basin is only one half of the size of the Upper Zambezi watershed the parameter value of k_1 is twice as big. This supports the conclusion that the water is drained quickly from the surface to the river and therefore losses are low.

While the parameters k_2 and k_4 show similar values for the Upper Zambezi basin and the Kafue river, they are much higher for the Luangwa river. This correlates well with

HESSD
7, 8809–8835, 2010

the generally steeper slopes in the Luangwa basin where water flows faster. Apparently the flow is attenuated by the wetlands in the Kafue and Upper Zambezi basins.

The performance of the model running in the deterministic mode is illustrated in Fig. 5 and compared to the reference method. The modeled discharge agrees in general quite well with the measured flows. For all the applied models the root mean squared error (RMSE) and the Nash-Sutcliffe efficiency are calculated (Tables 2 and 3). The model developed gives better results than the reference method for the Upper Zambezi and the Kafue River basin where both the Nash-Sutcliffe efficiency and the RMSE are slightly higher or lower, respectively. It is clearly visible that the flood maxima are reproduced much better than in the reference method. Obviously the inclusion of rainfall information is most beneficial for the maxima as the correlation between BWI and rainfall deteriorates for large precipitation events. However, for the Luangwa river the model performance was not satisfactory when running in the deterministic mode. It even showed a slightly poorer performance than the reference method which also does not allow to model the situation adequately.

Due to the parameter uncertainty the error band becomes large especially in the wet season. This uncertainty is mostly attached to the model parameter k_1 since with a high rainfall amount a slight change in the parameter can greatly affect the amount of water which is routed to the system.

A drawback for the testing of the method is the short time period over which data are available. The model relies on soil moisture data, on rainfall data and on measured discharge. The overlap of these three datasets dictates the longest continuous time span that can be modeled. Eventually it is only possible to test the model on a period of a bit more than six years, for the Upper Zambezi catchment even less. For this reason a full validation of the model was not possible. The available data were used to obtain a stable calibration.

For the successful application of the model for real-time prediction it does not necessarily have to be mechanistically correct but needs to reflect the correct tendency. When operating on-line in adaptive mode the quality of the forecast is of interest. The length of the forecast period is defined by the shortest time lag ($\Delta\tau$) in the model. The ensemble of the forecast can be represented by the ensemble mean and the confidence interval. As time approaches the time of prediction for a certain timestep the error generally gets smaller (Fig. 6). This statement is supported by the analysis of the RMSE and the Nash-Sutcliffe efficiency (Tables 2 and 3). While the prediction for the maximum forecast time shows the highest RMSE and lowest coefficient of efficiency, the model prediction gets significantly more accurate for shorter forecast periods. Again the absolute error of the prediction is much higher in the wet season. Whereas the relative error is especially high during ascending and receding flows (Fig. 6).

These results show clearly that the model presented is capable of providing useful discharge forecasts in semi-arid river basins. Yet this model can not be applied on every river since its model structure is not designed to reproduce the processes in watersheds with a relatively low storage volume and a quick response to rainfall events. The Soil Water Index (SWI) which was used to calculate the BWI assumes a uniform soil thickness everywhere. The actual thickness of the soil in a river basin has not a big influence on the model results. The spatial variability of the soil thickness however, has a huge influence on the results because certain areas with a relatively thin soil layer can suddenly dominate the behavior of the system.

The application of the model provides a seamless integration of remote sensing products. With only four parameters and a simple conceptual formulation this model is applicable to a class of watersheds which comply with certain characteristics. All data used are developed to an operational standard. Therefore the user does not have to undertake extensive data processing. This model is especially suited for use in a real-time modeling framework. More and more data from the newer satellite systems will be available in real-time. A higher temporal and/or a higher spatial resolution can greatly improve modeling efforts.

A higher spatial resolution of the data would allow a higher spatial resolution of the model. Since the BWI and the rainfall are averaged over the whole area, the runoff

HESSD
7, 8809–8835, 2010

processes are also averaged. The spatial variability of the different runoff processes is completely neglected. If heavy convective rainfall is occurring in an area with a high soil moisture a peak in the runoff should be observed. The model however, will overestimate the infiltration into the soil dramatically. Wagner et al. (2007) showed the usefulness of high resolution soil moisture data from the Envisat ASAR instrument in hydrological modeling. A higher temporal resolution of soil moisture data can allow models to account for the usually high temporal variability of the soil water content.

5 Conclusions

Hydrological modeling under data scarce conditions remains a big challenge. Recent developments offer promising opportunities to advance in this field. On one hand real-time modeling techniques allow the assimilation of data in a model, updating the modeled system state every time observation data are available. On the other hand techniques for extracting information on the hydrological cycle from remote sensing data have advanced in the past few years. While some years ago the satellite systems were designed to gather as many types of data as possible in order to provide the scientific community with data that can be exploited in several ways, nowadays satellite missions are designed for a specific purpose. Especially for the retrieval of soil moisture several satellite missions have been deployed recently or will be launched in the near future.

Radar scatterometer data were found especially promising for the use in hydrological modeling where the soil moisture is one of the most important parameters. Since the radar signal penetrates only the top few centimeters of the soil, hence only giving information on the surface soil moisture, the water content in the soil column has to be modeled. The simple two-layer model used to generate the SWI produces data which are appropriate to be used as input data for a conceptual model. Since rainfall is one important driver of soil moisture a conceptual model should also utilize rainfall data.

The prediction framework presented in this paper exploits the available data sets on rainfall and soil moisture. The relatively simple model consisting of two reservoirs, for the surface water and the subsurface water, and an infiltration process based on the soil moisture shows good performance. Especially in watersheds where the storage of water in the soil is of high importance the model predictions are accurate. In the Luangwa river basin which is dominated by steep slopes and quick runoff formation the model performance is not satisfactory.

Running the model in real-time with a data assimilation procedure provides short term forecasts which can be used for a wide variety of applications. To manage a river basin system such a forecast is beneficial since the discharge expected for the next few weeks can be quantified. Releases for power production, irrigation water demands or ecological flood releases can be planned based on this information.

If water management options for the distant future have to be assessed the described model is not suitable because it is not physically based. Due to the relatively long time step flood forecasting is also not possible. If the quality of the input data is greatly improved flash flood forecasting could eventually be an option. But further research is necessary to improve the quality of the data and to develop more sophisticated hydrological models tailored to use remotely sensed soil moisture data.

Acknowledgements. The soil moisture data were kindly provided by the Institute of Photogrammetry and Remote Sensing at the Vienna University of Technology. The discharge data of the three rivers were provided by the Department of Water Affairs, Lusaka, Zambia. This research is funded by the Swiss National Science Foundation under project K-21K1-120266.

References

Aubert, D., Loumagne, C., and Oudin, L.: Sequential assimilation of soil moisture and streamflow data in a conceptual rainfall-runoff model, J. Hydrol., 280, 145–161, doi:10.1016/S0022-1694(03)00229-4, 2003. 8811

Baghdadi, N., Cerdan, O., Zribi, M., Auzet, V., Darboux, F., El Hajj, M., and Kheir, R. B.: Operational performance of current synthetic aperture radar sensors in mapping soil surface

characteristics in agricultural environments: application to hydrological and erosion modelling, Hydrol. Process., 22, 9–20, doi:10.1002/hyp.6609, 2008. 8814
Brocca, L., Melone, F., Moramarco, T., and Morbidelli, R.: Spatial-temporal variability of soil moisture and its estimation across scales, Water Resour. Res., 46, W02516, doi:10.1029/2009WR008016, 2010. 8813
Ceballos, A., Scipal, K., Wagner, W., and Martinez-Fernandez, J.: Validation of ERS scatterometer-derived soil moisture data in the central part of the Duero Basin, Spain, Hydrol. Process., 19, 1549–1566, doi:10.1002/hyp.5585, 2005. 8814, 8819
Crow, W. T. and Ryu, D.: A new data assimilation approach for improving runoff prediction using remotely-sensed soil moisture retrievals, Hydrol. Earth Syst. Sci., 13, 1–16, doi:10.5194/hess-13-1-2009, 2009. 8811
Evensen, G.: Sequential Data Assimilation With A Nonlinear Quasi-Geostrophic Model Using Monte-Carlo Methods To Forecast Error Statistics, J. Geophys. Res.-Oceans, 99, 10143–10162, 1994. 8811
Herman, A., Kumar, V. B., Arkin, P. A., and Kousky, J. V.: Objectively determined 10-day African rainfall estimates created for famine early warning systems, Int. J. Remote Sens., 18, 2147–2159, 1997. 8816, 8819
Kerr, Y., Waldteufel, P., Wigneron, J.-P., Martinuzzi, J., Font, J., and Berger, M.: Soil moisture retrieval from space: the Soil Moisture and Ocean Salinity (SMOS) mission, IEEE T. Geosci. Remote, 39, 1729–1735, doi:10.1109/36.942551, 2001. 8812
Kitanidis, P. K. and Bras, R. L.: Real-Time Forecasting With a Conceptual Hydrologic Model 1. Analysis of Uncertainty, Water Resour. Res., 16, 1025–1033, doi:10.1029/WR016i006p01025, 1980a. 8811
Kitanidis, P. K. and Bras, R. L.: Real-Time Forecasting With a Conceptual Hydrologic Model 2. Applications and Results, Water Resour. Res., 16, 1034–1044, doi:10.1029/WR016i006p01034, 1980b. 8811
Marquardt, D.: An algorithm for least-sqares estimation of nonlinear parameters, J. Soc. Ind. Appl. Math., 11, 431–441, 1963. 8818
McLaughlin, D.: An integrated approach to hydrologic data assimilation: interpolation, smoothing, and filtering, Adv. Water Resour., 25, 1275–1286, 2002. 8811
Naeimi, V., Bartalis, Z., and Wagner, W.: ASCAT Soil Moisture: An Assessment of the Data Quality and Consistency with the ERS Scatterometer Heritage, J. Hydrometeorol., 10, 555–563, doi:10.1175/2008JHM1051.1, 2009. 8812

HESSD
7, 8809–8835, 2010

Hydrological real-time modeling using remote sensing data

P. Meier et al.

Nash, J. and Sutcliffe, J.: River flow forecasting through conceptual models part I – A discussion of principles, J. Hydrol., 10, 282–290, 1970. 8818
Piles, M., Entekhabi, D., and Camps, A.: A change detection algorithm for retrieving high-resolution soil moisture from SMAP radar and radiometer observations, IEEE T. Geosci. Remote, 47, 4125–31, 2009. 8812
Scipal, K., Scheffler, C., and Wagner, W.: Soil moisture-runoff relation at the catchment scale as observed with coarse resolution microwave remote sensing, Hydrol. Earth Syst. Sci., 9, 173–183, doi:10.5194/hess-9-173-2005, 2005. 8814, 8815, 8817, 8818, 8834
Thiemann, M., Trosset, M., Gupta, H., and Sorooshian, S.: Bayesian Recursive Parameter Estimation For Hydrologic Models, Water Resour. Res., 37, 2521–2535, doi:10.1029/2000WR900405, 2001. 8811
Verstraeten, W., Veroustraete, F., van der Sande, C., Grootaers, I., and Feyen, J.: Soil moisture retrieval using thermal inertia, determined with visible and thermal spaceborne data, validated for European forests, Remote Sens. Environ., 101, 299–314, doi:10.1016/j.rse.2005.12.016, 2006. 8813
Wagner, W., Lemoine, G., Borgeaud, M., and Rott, H.: A study of vegetation cover effects on ERS scatterometer data, IEEE T. Geosci. Remote, 37, 938–948, doi:10.1109/36.752212, 1999a. 8811, 8814
Wagner, W., Lemoine, G., and Rott, H.: A method for estimating soil moisture from ERS scatterometer and soil data, Remote Sens. Environ., 70, 191–207, 1999b. 8814
Wagner, W., Bloeschl, G., Pampaloni, P., Calvet, J.-C., Bizzarri, B., Wigneron, J.-P., and Kerr, Y.: Operational readiness of microwave remote sensing of soil moisture for hydrologic applications, Nord. Hydrol., 38, 1–20, doi:10.2166/nh.2007.029, 2007. 8813, 8823
Western, A. W., Zhou, S.-L., Grayson, R. B., McMahon, T. A., Blschl, G., and Wilson, D. J.: Spatial correlation of soil moisture in small catchments and its relationship to dominant spatial hydrological processes, J. Hydrol., 286, 113–134, doi:10.1016/j.jhydrol.2003.09.014, 2004. 8813

HESSD
7, 8809–8835, 2010

Hydrological real-time modeling using remote sensing data

P. Meier et al.

HESSD
7, 8809–8835, 2010

Hydrological real-time modeling using remote sensing data

P. Meier et al.

Table 1. Estimated parameters for the three sub-basins and the 95% confidence interval for each parameter.

	Upper Zambezi	Kafue River	Luangwa River
Δt_S	40 d	20 d	10 d
Δt_{GW}	100 d	70 d	50 d
k_1 $(\times 10^{-5})$	4.22 ± 1.13	5.00 ± 0.99	10.44 ± 3.68
k_2	0.22 ± 0.09	0.29 ± 0.09	0.68 ± 0.46
k_3 $(\times 10^{3})$	32.23 ± 6.41	5.61 ± 1.32	18.06 ± 5.58
k_4	0.15 ± 0.03	0.13 ± 0.03	0.35 ± 0.09

HESSD
7, 8809–8835, 2010

Hydrological real-time modeling using remote sensing data

P. Meier et al.

Table 2. RMSE of the different model runs for all the sub-basins (in $m^3\,s^{-1}$).

	Upper Zambezi	Kafue River	Luangwa River
Deterministic	269.3	99.5	513.7
Adaptive mode			
$\Delta t = 40$ d	281.5		
$\Delta t = 30$ d	265.1		
$\Delta t = 20$ d	238.8	70.5	
$\Delta t = 10$ d	199.1	59.8	483.6
$\Delta t = 0$ d	131.4	46.5	412.6
Reference	285.0	103.8	502.6

Table 3. Nash-Sutcliffe efficiency of the different model runs for all the sub-basins.

	Upper Zambezi	Kafue River	Luangwa River
Deterministic	0.90	0.82	0.74
Adaptive mode			
$\Delta t = 40\,\mathrm{d}$	0.85		
$\Delta t = 30\,\mathrm{d}$	0.87		
$\Delta t = 20\,\mathrm{d}$	0.90	0.84	
$\Delta t = 10\,\mathrm{d}$	0.93	0.88	0.68
$\Delta t = 0\,\mathrm{d}$	0.98	0.96	0.80
Reference	0.88	0.80	0.75

HESSD
7, 8809–8835, 2010

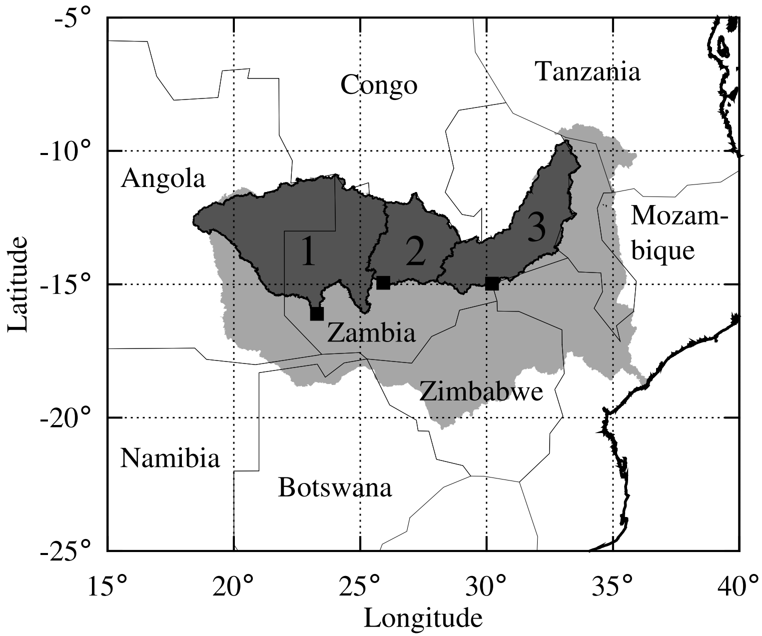

Fig. 1. Overview of the Zambezi River Basin (light gray) and the three watersheds where the model is applied. 1: Upper Zambezi; 2: Kafue River; 3: Luangwa River. The outlets of the watersheds are marked (■).

HESSD

7, 8809–8835, 2010

Hydrological real-time modeling using remote sensing data

P. Meier et al.

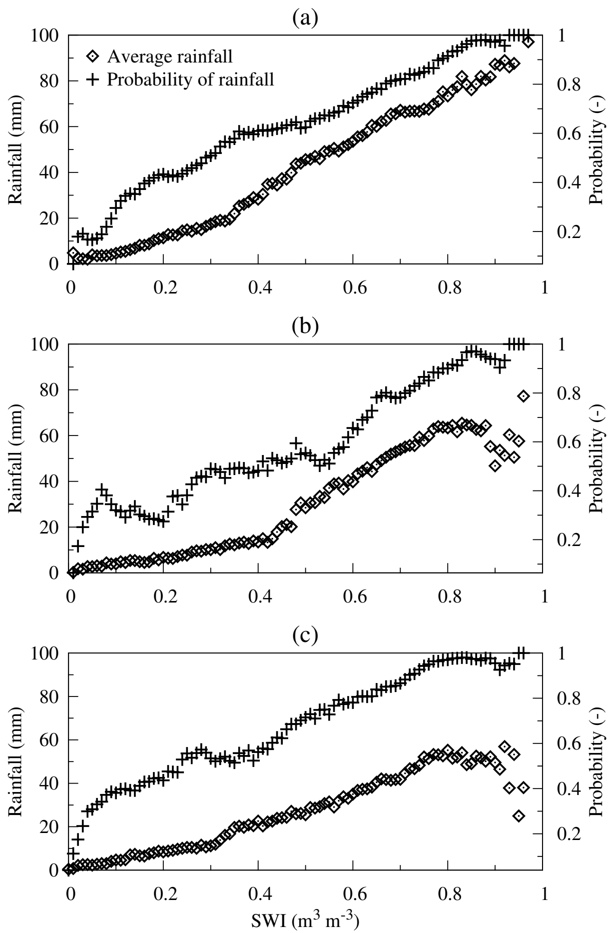

Fig. 2. The probability of a rainfall event given a Soil Water Index (SWI) class and the average rainfall amount for the same classes for the three watersheds Upper Zambezi **(a)**, Kafue River **(b)** and Luangwa River **(c)**.

HESSD

7, 8809–8835, 2010

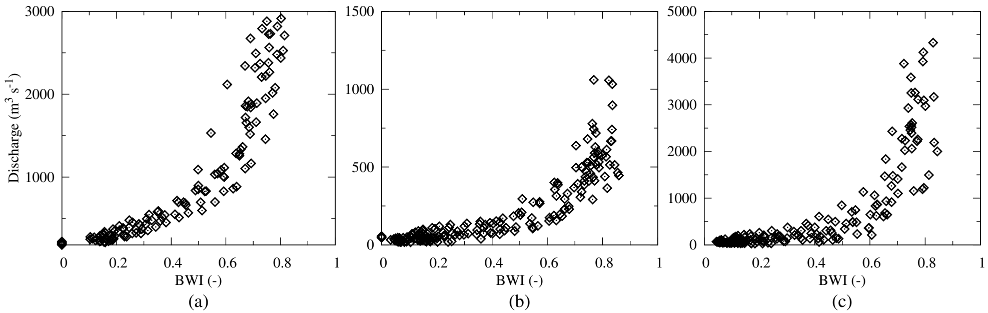

Fig. 3. Correlation between BWI and discharge shifted by the time lag (Δt) which resulted in the best correlation. **(a)** Upper Zambezi: $\Delta t = 60$ d; **(b)** Kafue River: $\Delta t = 30$ d; **(c)** Luangwa River: $\Delta t = 0$ d.

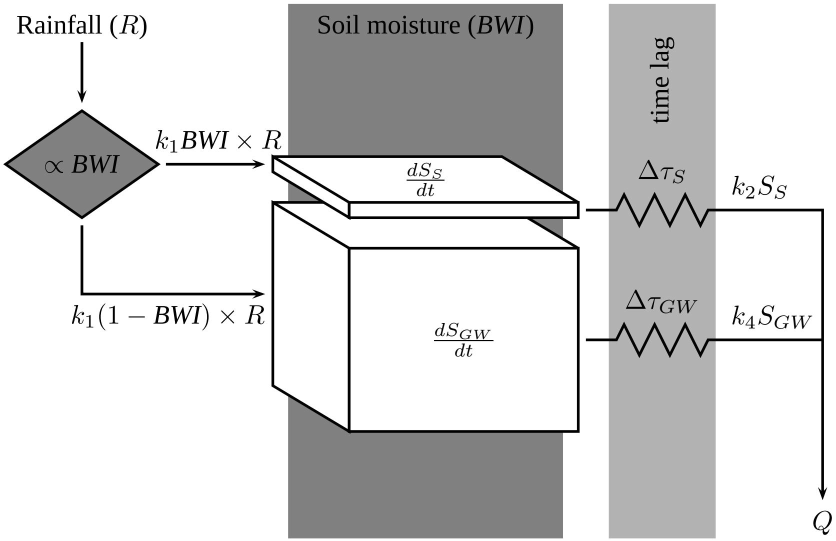

Fig. 4. Structure of the conceptual hydrological model.

HESSD
7, 8809–8835, 2010

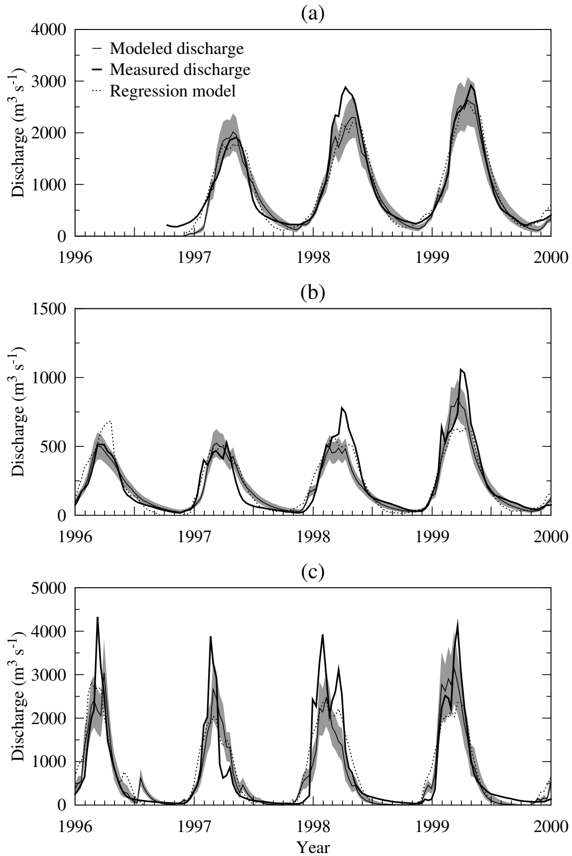

Fig. 5. The modeled discharge (thin line) including the 95% confidence interval compared to the measured discharge (thick line) for the three watersheds Upper Zambezi **(a)**, Kafue River **(b)** and Luangwa River **(c)**. For comparison the results of the regression model by Scipal et al. (2005) are indicated (dashed line).

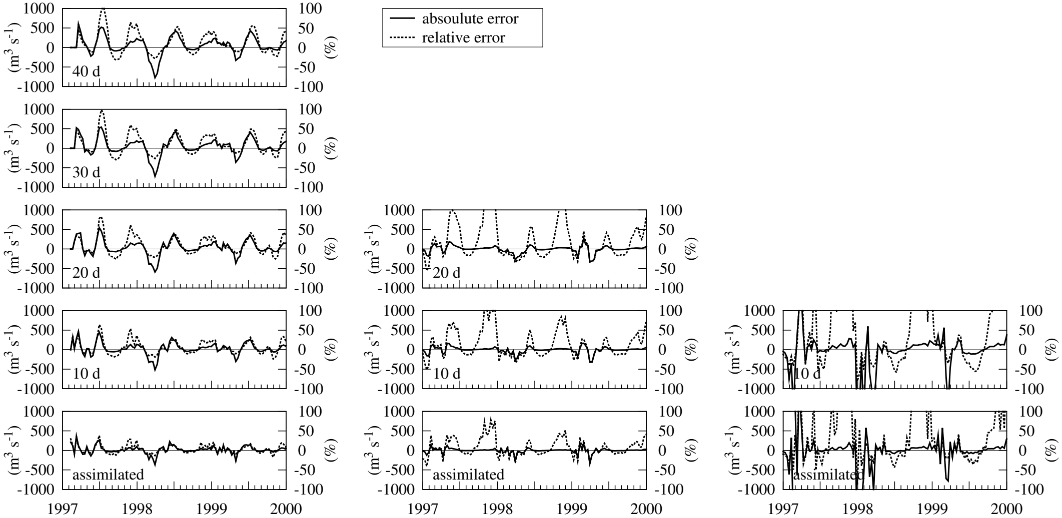

Fig. 6. Absolute and relative forecast error for the Upper Zambezi (left), the Kafue (center) and the Luangwa watersheds (right) for the different forecast periods and the assimilation step.

HESSD
7, 8809–8835, 2010

Hydrological real-time modeling using remote sensing data

P. Meier et al.